J. Chil. Chem. Soc., 63, Nº 4 (2018)

Mn^{2+}-COMPLEXES OF N,O-DIHYDRAZONE: STRUCTURAL STUDIES, INDIRECT BAND GAP ENERGY AND CORROSION INHIBITION ON ALUMINUM IN ACIDIC MEDIUM

AYMAN H. AHMED[1,2], A.M. HASSAN[2], HOSNI A. GUMAA[2], BASSEM H. MOHAMED[2], AHMED M. ERAKY[2]*

[1]*Chemistry Department, College of Science and Arts, Jouf University, Gurayat, Saudi Arabia.*
[2]*Department of Chemistry, Faculty of science, Al-Azhar University, Nasr City, Cairo, Egypt.*

ABSTRACT

Mononuclear manganese complexes of dihydrazone derived from the condensation of oxaloyldihydrazide with 2-hydroxynaphthaldehyde and 2-methoxybenzaldehyde have been synthesized. The hydrazone Schiff base ligands and their chelates were characterized on the basis of their elemental analyses, spectral (UV-Vis., IR, mass, $^{1}H/^{13}C$ NMR), magnetism, ESR and thermal (TGA) measurements. The dihydrazone has been suggested to coordinate to the metal center in bi-dentate manner forming 1:1[M:L] complex. The complexes are suggested to have tetrahedral/octahedral stereochemistry. Optical transmission spectra were recorded in the range 190–2100 nm and optical band gap energy was determined. The band gap energy (E_g) for all separated compounds lies in the range of semiconductors. On the other hand, the inhibition and adsorptive properties of the ligands for the corrosion of aluminum in 1 M HCl solutions were studied using traditional weight loss measurements. The results revealed that bis(2-methoxy-benzaldehyde)oxaloyldihydrazone has a greater inhibition than bis(2-hydroxy-1-naphthaldehyde)oxaloyldihydrazone. The adsorption of the inhibitors on metal surface was found to be spontaneous first order reaction and consistent well with the mechanism of physical adsorption. The adsorption data fitted well to Freundlich, Langmuir and Frumkin adsorption isotherms.

Keyword: Metal complexes; Hydrazones; Structure elucidation; Corrosion.

INTRODUCTION

Hydrazones are characterized by the presence of the triatomic grouping C=N-N-. They can be considered as Schiff bases derived from acid hydrazides. The most important property of hydrazones is their high physiological activity [1]. They are important for drug design, organocatalysis and also for the syntheses of heterocyclic compounds [2]. Furthmore, hydrazones and their transition metal complexes have shown their applications in biological systems, analytical chemistry and as catalysts [3]. In the context of complexation, hydrazones (derived from o-hydroxy aldehydes) containing amide, azomethine and phenol functions are recently recognized as polyfunctional ligands which can react with metal ions either in keto form and enol form [4]. Extensive studies have revealed that the lone pair on the nitrogen of the azomethine group (-CH=N-) is responsible for their chemical and biological activities [5-7]. Although a series of transition metal complexes of hydrazones [M= Cu(II), Ni(II), Mn(II), Pd(II), Co(II), V(IV) and ruthenium(II)] were synthesized and characterized [8-15], a survey of literature revealed that only a few metal complexes of oxaloyldihydrazone have been investigated [16-18]. The reason of that arises from their poor solubility. Oxaloyldihydrazones are only soluble in high polar solvents such as dimethylformamide (DMF) and dimethylsulfoxide (DMSO) and this requires much effort to isolate them or their complexes in pure form. Interestingly, some hydrazone complexes have been accommodated in zeolite-Y by alternative methods and the structures of the solid complexes inside the zeolite were sustained by variety of physico-chemical techniques and spectroscopic studies [19-24].

Inhibitor applications often play an important role in oil extraction and processing industries, heavy industrial manufacturing, water treatment facility, water-containing hydraulic fluids, water treatment chemicals, engine coolants, ferrous metal cleaners, automatic transmission fluids, automotive component manufacture, cutting fluids etc. to minimize localized corrosions and unexpected sudden failures. Acid solutions are widely used in industry, the most important fields of application being acid pickling and industrial acid cleaning due to the general aggressively of acid solutions; thus enhancing corrosive attack on metallic materials. The most important aspect of inhibition normally considered by corrosion scientists is the relation between molecular structure and corrosion inhibition efficiency. Most of the well-known acid inhibitors are organic compounds containing π bonds, phosphorus, sulfur, oxygen and nitrogen as well as aromatic rings in their structure which are the major adsorption centers [25]. Heteroatoms such as nitrogen, oxygen and sulfur are capable of forming coordinate covalent bond with metal owing to their free electron pairs and thus acting as inhibitors. Unfortunately, many common corrosion inhibitors employed in aqueous media are health hazards [28].

In view of the significant role played by the hydrazones and their metal complexes in various fields, we motivated to synthesize and characterize of two oxaloyldihydrazones and their Mn^{2+} complexes. The band gap energy of the investigated compounds has been estimated to describe their optical and electronic properties. The work was also undertaken to explore the use of selected oxaloyldihydrazones as corrosion inhibitors for aluminum in hydrochloric acid solution where some kinetic and thermodynamic parameters were calculated and discussed.

EXPERIMENTAL

Chemicals and Equipments

The aldehydes were obtained from Merck Company. Manganese (2+) acetate, diethyl oxalate, hydrazine monohydrate were purchased from Sigma-Aldrich. Oxalicdihydrazide was prepared by reacting diethyloxalate (1 mol) with hydrazine hydrate (2 mol) [10], (Exp/Lit. m.p = 240/240 °C). Other employed chemicals and solvents were of highest purity and used without further purification. Elemental analyses (CHNM), spectral (UV-Vis., FT-IR, Mass) and thermal (TG) measurements were executed as mentioned elsewhere [29,10]. The NMR spectra were recorded on a Varian mercury VX-300 NMR spectrometer. ^{1}H spectra were run at 300 MHz and ^{13}C spectra were run at 75.46 MHz in dimethylsulphoxide (DMSO-d_6). Tetramethylsilane (TMS) was used as an internal reference and chemical shifts are quoted in δ (ppm). Magnetic moments (μ_{eff}) of the samples were measured at room temperature (RT) using Faraday's method. The ESR spectra of the complexes were recorded in powder form at room temperature using Bruker-EMX-(X-bands-9.7 GHZ) spectrometer with 100 KHZ frequency, microwave power 1.008 mW and modulation/amplitude of 4 GAUSS at national center for radiation research and technology, Egypt. The band gap energy (E_g) of product compounds was calculated according to Tauc's equations [30,31]. Corrosion test was performed on freshly prepared sheet of aluminum of chemical compositions (wt %) Ni (0.006), Pb (0.01), Zn (0.003), Cu (0.002), Fe (0.27) and Al (99.71). The metal specimens were prepared, degreased and cleaned as previously described [10].

Synthesis of oxaloyldihydrazone ligands

The dihydrazone ligands; bis(2-hydroxynaphthaldehyde) oxaloyldihydrazone (L_1) and bis(2-methoxybenzaldehyde)oxaloyldihydrazone (L_2) were prepared using the same procedure described in Ref. 10 as follows. Aqueous methanolic solution of oxaloyldihydrazine was mixed with absolute methanolic solution of the selected aldehydes (maintaining the molar ratio at 1:2) in hot condition. The reaction mixture was heated for about 3 hours accompanied by stirring. The precipitate was separated out on concentrating the solution to half of its volume and cooling. Afterwards, the isolated compound was filtered, recrystallized from DMF-$MeOH_{aq}$ mixed solvent, washed thoroughly by acetone and then dried in an electric oven at 80 °C for 2 h. The molecular structure of the resulting hydrazones was confirmed by elemental analyses, (IR, mass and $^{1}H/^{13}C$ NMR) spectroscopy (Table 1, 2). The mass spectral data of the ligands (L_1, L_2) are displayed in Fig. 1 and the obtained M^+ values are set out in Table 1. Mass spectrum of the bis(2-hydroxy-1-naphthaldhyde)oxaloyldihydrazone (L_1) revealed ion peaks at m/e = 427 (20%, molecular peak, ($C_{16}H_{14}N_4O_4$)), 410 (25%, $M^+(C_{24}H_{18}N_4O_3)$), 270 (21%, $M^+(C_{13}H_{10}N_4O_3)$), 157 (21.2%, $M^+(C_{11}H_9O)$), 257 (50%, $M^+(C_{13}H_{10}N_3O_3)$), 242 (40%, $M^+(C_{13}H_9N_2O_3)$), 175 (71%, $M^+(C_{11}H_9NO)$), 141 (4%, $M^+(C_{11}H_9)$), 128

e-mail: ayman_haf532@yahoo.com

(37%, $M^+(C_{10}H_8)$), 79 (40%, $M^+(C_6H_8)$), 64.95 (71%, $M^+(C_5H_5)$) and 50 (100%, base peak, $M^+(C_4H_4)$. Mass spectrum of the bis(2-methoxybenzaldehyde) oxaloyldihydrazone (L_2) exhibited ion peaks at m/e = 356.45 (33%, molecular peak, ($C_{18}H_{18}N_4O_4$)), 247.35 (26%, $M^+(C_{11}H_{11}N_4O_3)$), 217.2 (62%, $M^+(C_{10}H_9N_4O_2)$), m/e = 50 (100%, base peak, $M^+(C_4H_4)$), 234.2 (42%, $M^+(C_{10}H_{10}N_4O_3)$), 202 (25%, $M^+(C_{10}H_9N_2O_3)$), 176.5 (60%, $M^+(C_9H_9N_2O_2)$), 149 (92%, $M^+(C_8H_9N_2O)$), 190.6 (46%, $M^+(C_9H_8N_3O_2)$), 175.55 (78%, $M^+(C_9H_7N_2O_2)$), 119.4 (53%, $M^+(C_7H_7N_2)$), 104.2 (51%, $M^+(C_7H_6N)$), 134.6 (82%, $M^+(C_8H_8NO)$), 107.15 (52%, $M^+(C_7H_8O)$), m/e = 90.6 (75%, $M^+(C_7H_6)$), 77.05 (86%, $M^+(C_6H_6)$) as well as 66.65 (38%) corresponds to $M^+(C_5H_6)$. The spectral data assured the chemical formula of the ligands as well the correct molecular weights.

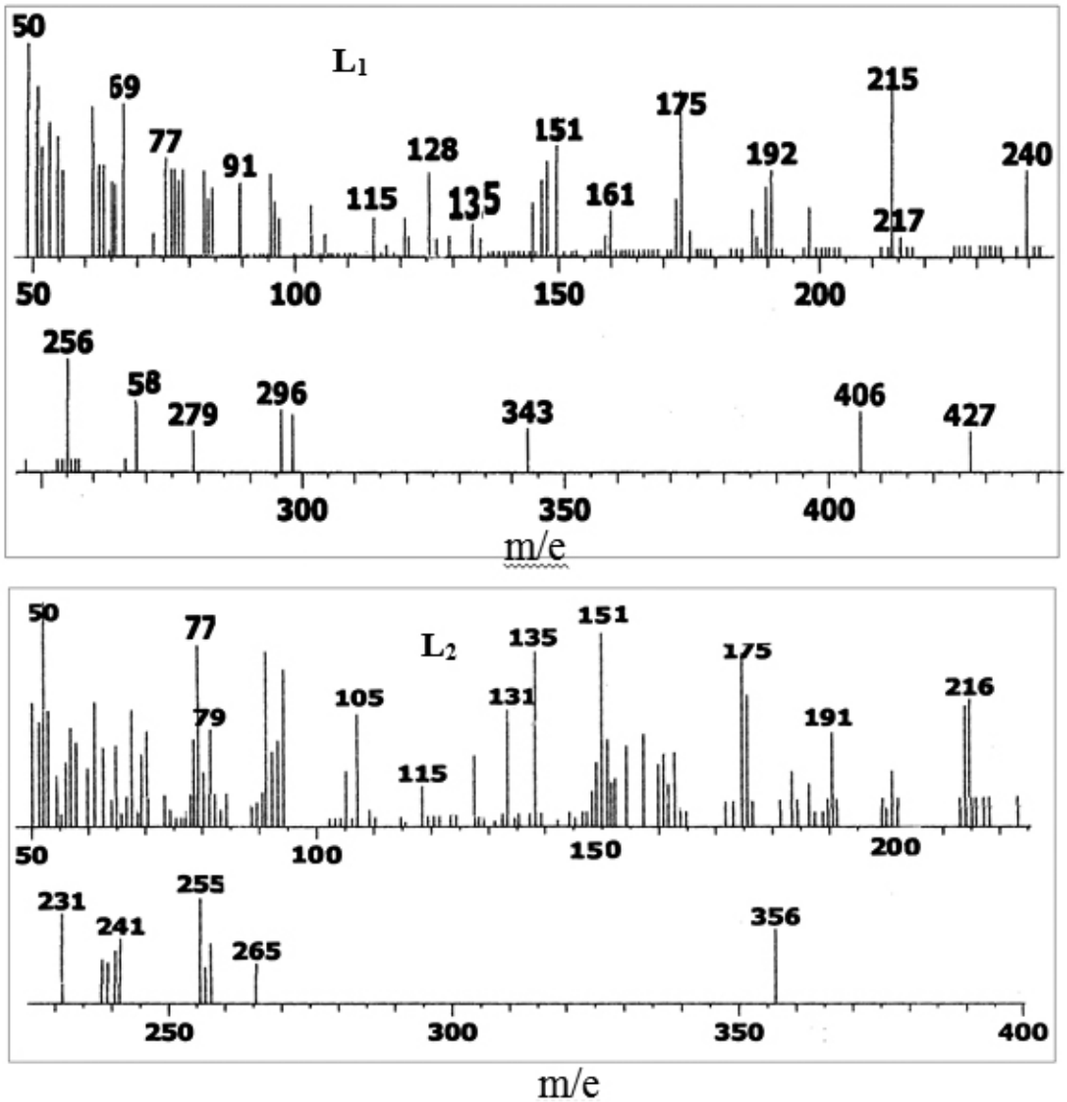

Fig.1. Mass spectra of L_1 and L_2.

Synthesis of solid complexes

Manganese (2+) complexes were prepared by literature method [10]. Dihydrazone (1 mmol) were dissolved first in 20 ml DMF and then 50 ml methanol was added. The obtained solution was added slowly to a 20 ml methanolic solution of Mn (2+) acetate in 1:2 molar ratio. The resulting mixture was refluxed for 4 hours and then reduced to 30 cm^3 by gentle heating. The desired product obtained on cooling down to room temperature was filtered off, washed vigorously in beaker with successive portions of hot solvents (dimethylformamide, methanol and acetone, respectively) and dried in an electric oven at 80 °C for 8 hrs.

Solutions

The aggressive solutions, 1 M HCl, were prepared by dilution of analytical grade HCl with distilled water. Stock solutions of the inhibitors were prepared in DMF. All test solutions contained 10 ml (20 vol.%) of DMF to ensure solubility. The concentrations of the used inhibitors (L_1 and L_2) were 5×10^{-4}, 1×10^{-4}, 5×10^{-5} and 1×10^{-5} M.

Gravimetric measurements

A simple test for measuring corrosion is the gravimetric method (weight loss). The method involves exposing a clean weighed piece of the metal or alloy to the corrosive environment for a specified time followed by cleaning to remove corrosion products and weighing the piece to determine the loss of weight.

A previously weighed metal (aluminum) was completely immersed in 50 ml of the test solution (1M HCl) in an open beaker. The beaker was maintained at a temperature of 301 K. The aluminum coupons were suspended in the beaker with the help of glass hooks. The coupons were withdrawn from the test solution at 1 h interval progressively for 4 h, dipped into saturated

ammonium acetate solution to terminate the corrosion reaction, washed by scrubbing with a light brush, rinsed in acetone and finally dried in an oven at 80 ˚C before reweighing. The difference in weight in grams was taken as the

$$W = W_i - W_f$$

total weight loss (W) [32].

Where: W_i and W_f are the initial and final weights for aluminum, respectively.

The corrosion rate, ρ (in $gm.cm^{-2}.min^{-1}$) for aluminum at different concentrations of the acid was determined using the following equation [33]:

$$\rho = \frac{W}{A \times t}$$

Where: W = weight loss to the nearest 0.0001gm, A = area of specimen to the nearest 0.01 cm^2 (2 × area of one face) and t = exposure time (minutes).

The inhibition efficiency (%η) for each inhibitor and the degree of surface coverage (θ) were calculated using the equations [33]:

$$\eta\% = \left[1 - \frac{\rho_1}{\rho_2}\right] \times 100$$

$$\theta = 1 - \frac{\rho_1}{\rho_2}$$

Where ρ_1 and ρ_2 are the corrosion rates in the presence and absence of inhibitor, respectively.

Table 1: Analytical, physical and spectroscopic data of the oxaloyldihydrazones and their related Mn(II) complexes.

Compound	Symbol	M.p(ºC) Color	Found(calcd.)%				^{1}H-NMR/ ^{13}C-NMR Chemical shift (δ_{ppm})	$\mu_{eff.}$ 4Å/ 6A	M^+ Found/ calcd.	E_g (eV)	$g_\perp$	$g_{//}$	g_{av}
			C	H	N	M							
$C_{24}H_{18}N_4O_4$	L_1	>300 Yellow	68.1 (67.7)	5.3 (4.3)	12.9 (13.2)	- -	12.76(NH, s), 12.57(OH, s), 9.74(CH=N, s), 6.5-8.5 (aromatic protons, m)/ 158.4,158.3, 157.1,155.7, 150.4,149.7, 133.2, 132.5, 128.9, 127.8, 123.6, 120.5,118.8	-	427.1/ 426.4	3.06	-	-	-
$C_{18}H_{18}N_4O_4$	L_2	>300 White	59.2 (61)	5.8 (5.1)	15.7 (15.8)	- -	12.3(NH, s), 11.9(OH, s), 8.95(CH=N, s), 6.8-8.5(aromatic protons, m), 3.93(OCH_3, s)/156.2, 148.7, 158.1, 132.1, 125.8, 122.0, 120.9, 55.7.	-	355.0/ 354.4	3.42	-	-	-
[Mn(L_1-H) (H_2O)$_2$].0.5 H_2O	I	>300 Brown	54.2 (54.9)	4.0 (4.2)	10.2 (10.5)	10.8 (10.7)	-	4.4/ 4.7	-	2.38	1.88	1.930	1.9
[Mn(L_2-2H) ($OAc)_2(DMF)_2$]	II	>300 Yellowish	49.1 (49.9)	5.2 (5.7)	12.1 (12.5)	9.2 (8.2)	-	5.1/ 4.7	-	3.39	1.85	1998	1.9

RESULTS AND DISCUSSION

The analytical and spectroscopic data as well as physical properties of the ligands and coordination compounds are listed in Tables 1,2. The results show that the dihydrazone ligands coordinate to the manganese ion in a 1:1 molar ratio. The prepared complexes are non-hygroscopic, soluble in strong polar solvents such as in DMF and DMSO but insoluble in H_2O, $CHCl_3$, CCl_4, alcohol, acetone, ether as well as benzene. The calculated and found percentages of elements (CHNM%) point out that the compositions of the isolated complexes harmonize with the proposed formulae.

Stereo chemical structure of Mn^{2+}-complexes

IR Spectra

The comparative IR spectral study of the dihydrazones and their manganese (2+) complexes reveals the coordination mode of the ligands during complex formation. The important frequencies with their possible assignments are listed in Table 1.

Free ligand: Prepared oxloyldihydrazones can be represented either in the trans- (staggered) or cis- (anti-cis- or syn-cis-) configuration as revealing in Fig. 2 [34]. The structures of the ligands were authenticated on the basis: (1) the ν(C=N) was observed in the IR spectra of the two ligands at 1600-1618 cm^{-1} indicating the interaction of dihydrazide with the aldehyde. (2) The bands at 3476, 3166 and (1705(m) +1660(v.s) cm^{-1} are attributed to $\nu(OH)_{naphthoic}$, ν(NH) and ν(C=O) for L_1, respectively, meanwhile, L_2 which does not contain o-hydroxy group revealed ν(NH) at 3202 cm^{-1} and ν(C=O) at 1653 cm^{-1}. (3) Both ν(C=O) and ν(NH) are observed concurrently in the IR spectra of the two ligands giving an important reflection to the existence of keto forms. (4) Appearance of ν(C=O) as two bands in case of L_1 (1705, 1660 cm^{-1}) and one band for L_2 (1653 cm^{-1}) refers to the mixture of [cis(syn/anti-cis-structure) + trans(staggered)-structure)] isomers for L_1 and trans (staggered) structure for L_2, respectively, (Fig. 2). This suggestion is assumed in the light of the field effect criteria where the cis isomer is absorbed at higher frequency than trans one [10]. The band observed at 1705 cm^{-1} characterized cis form while the other two bands located at 1660 and 1653 cm^{-1} indicated the presence of trans-form. Otherwise, NMR spectroscopy provides satisfactory agreement with this view as shown later. (5) The band observed at 3227 cm^{-1} (L_2) may concern $\nu(OH)_{enolic}$ in H-bond bonding with C=N. (6) The bands corresponding to ν(C-O) in the spectra of L_1 and L_2 were located at 1287 and 964 cm^{-1}, respectively [35,36]. (7) Also, each ligand contains bands in the regions 1400-1600 and one band at 700-800 cm^{-1} assignable to ν(C=C) and $\delta(CH)_{out\ of\ plane}$ of the aromatic ring, respectively.

Mn^{2+}-complexes: The IR spectra of the complexes (I, II) are depicted

in Table 2. Virtually, it is difficult to unambiguously assign the bands due to foundation of various groups e.g., C=O, C=N, N-C=O, NH, OH, ph ring, C-N and C-H which absorb in the overlapping regions. On examining the IR spectra of the complexes in comparison with those of the free ligands, the complexes structures are suggested based on the following evidences:

For I, the splitting of the azomethine band (1600, 1618 cm^{-1}) justifies the imparting of this group in coordination [37] where two dissimilar azomethine groups are presented, Fig. 3 [38]. One of them is coordinated with manganese while the other is free. This occurred due to the enolization of left or right half of the dihydrazone molecule assuming keto-enol skeleton. Existence of $\nu(OH)_{naphthoic}$ at 3342 cm^{-1} endorses this suggestion. Interestingly, the obscure of ν(NH) with noticeable of ν(C=O) at 1655 cm^{-1} upon chelation give a conclusive evidence to the coordination of metal ion with deprotonated NH group. Persistence of ν(C=O) as one band, 1655 cm^{-1} instead of two bands in L_1 with slightly change in its location agrees with the presence of the two oxygen atoms related to (O=C-C-OH) part, in trans direction. Doubtless the positive shift observed for ν(C-O) vibration (1287→1299 cm^{-1}) provides a clue to deprotonation of both phenolic (OH) groups during their coordination [6,36,39] but remarking $\nu(OH)_{naphthoic}$ at 3186 cm^{-1} points to the existence of naphthoic (OH) in H-bonding, Fig. 4. This can be explained on the basis of the deprotonation of one naphthoic (OH) group while the other is in H-bonding with C=N group.

Table 2: Significant IR and electronic absorption data of oxaloyldihydrazones and their manganese complexes.

Symbol	$\nu_{(OH)}$ naphthoic (enolic)	ν_{H2O}	ν_{NH}	ν_{C-H} aromatic (aliphatic)	$\nu_{C=O}$	$\nu_{C=N}$	ν_{C-O} naphthoic/ methoxy	ν_{C-OMe}	δ_{C-H} aromatic, out of plane	ν_{M-O} naphthoic / enolic (carbonyl/ methoxy)	λ_{max} (nm)/ assignments	Structure
L_1	3476 (-)	-	3166	3043 (2926)	1705 1660	1621	1287	-	741	-/- (-/-)	392(n-π*, C=N), 375(n-π*, C=O), 330(π -π*, C=N), 315(π -π*, C=O), 303(π -π*, Phenyl)	-
L_2	- (3227)	-	3202	3041 (2940)	1653	1600	-	964	760	-/- (-/-)	350(n-π*, C=N), 338(n-π*, C=O), 306(π -π*, C=N), 292(π -π*, C=O), 280(π -π*, Phenyl)	-
I	3186 (3342)	3379	-	3051 (2925)	1655	1618 1600	1299	-	745	567/- (-/-)	460 ($^6S\rightarrow{}^4G$) 425 ($^6S\rightarrow{}^4P$)	Tetra-hedral
II*	- (-)	-	3203	3040 (2936)	1652 strong	1600	-	964	761	-/- (-/640)	430/$^6A_{1g}\rightarrow{}^4T_{1g}$(G) 380/$^6A_{1g}\rightarrow{}^2T_{2g}$(G)	Octa-hedral

* *$\nu_{C=O}$ of DMF was observed at 1729 cm^{-1}, ν_{OAc} was observed at 1351and 1437 cm^{-1}*

In case of II and comparing with the IR spectrum of L_2 ligand, The mode of chelation is supported by following facts: (1) The remaining of the ν(NH), ν(C=N) and ν(C-OMe) at nearly the same position with disappearance of $\nu(M-O_{methoxy})$ excludes involvement of the above groups in bonding. The feature of the interesting band assigned to ν(C=O) is varied from strong to very strong relative to other neighbor bands indicating the coordination of the above group with manganese ion. Undoubtedly, the observation of C=O groups in the IR spectrum of II with obscure of ν(NH) band implies that the ligand prefers its keto form to coordinate with Mn^{2+} ion. DMF showed band at 1729 cm^{-1} assigned to the ν(C=O) stretch and this band is not observed in the free ligand [40].

Actually, the appearance of new M-O bands in both complexes (Table 3) asserts the formation of metal-ligand bond [41]. The broad bands within the range 3300–3450 cm^{-1} in the complex I are attributed to the presence of crystalline and coordinated water molecules. Besides, the two bands corresponding to ν_{as} and ν_s carboxylic modes of acetate group are shown at 1351 cm^{-1} and 1437 cm^{-1}, respectively. The larger difference between the above two frequencies [ν_{as}(OAc) and ν_s(OAc)] is an indicative of monodentate nature of acetato group [42]. Also, the slight changes in the positions of $\nu(C=C)_{ph}$ upon chelation are due to metal-ligand interaction.

^{1}H/^{13}C NMR Spectra

The spectra of the two investigated ligands (Table 1) contain signals at 6.5–8.5, 9.73, 8.95 12.8, 12.6, 12.3 and 3.9 ppm which are assigned to aromatic(L_1, L_2), azomethine (L_1), azomethine (L_2), -NH (L_1), naphthoic –OH (L_1), secondary -NH (L_2) and -OCH_3(L_2) protons [11], respectively. The disappearance of signals due to –OH and –NH protons, on D_2O exchange confirms to the assignment of signals in the ligand spectrum. In the spectrum of the L_1. the signal due to the naphthoic –OH protons appeared as a broad singlet suggesting its capability to establish intermolecular H-bonding with DMSO solvent. A probable existence of interamolecular hydrogen bonding between naphthoic -OH and CH=N group was ruled out owing to its appearance at normal position. The observation of δ(NH) with nonexistence of enolic OH in the same spectra (L_1) implies the ligand is present in the keto form. In the spectrum of the L_2, noticeable of δ(NH) at 12.29 ppm accompanied with very weak intensity of $\delta(OH)_{enolic}$ at 11.92 ppm infers domination of diketo form compared with dienol or keto-enol form. Surely, NMR spectroscopy can determine the skeleton of the oxaloydihydrazone. As reported in literature [41], if the dihydrazone exists in the syn-cis-configuration or staggered configuration, the δOH, δNH and δCH=N, resonances, each should appear as a singlet. However, the appearance of these signals in the form of six signals (doublet of doublet) indicates anti-cis (chair) configuration. Based on this supposition together with the obtained data it can be concluded that the two ligands are in conformity with syn-cis- or staggered configuration. But the IR information clearly indicates that the staggered configuration is well defined.

The ^{13}C NMR measurement was performed for the two ligands and the resulting data (Fig. 3, Table 1) correlate well with ^{1}H NMR spectra without discrepancies. The ^{13}C NMR spectroscopy data for L_1 gave resonances at 155.7 ppm for C=O, 149.7 ppm for C=N and 158.3, 132.5, 128.9, 127.8, 123.6 for Ar-C2, Ar-C4, Ar-C6, Ar-C5, Ar-C1, respectively, confirming a staggered symmetry for L_1. The greater number of lines than the carbon types in the proposed configuration may be recognized from the existence of some ligand molecules in diketo and/or dienol forms. ^{13}C NMR spectrum of L_2 was also in good conformance with ^{1}H NMR assuming a keto-keto form (staggered structure). The spectrum showed three distinct peaks assigned to C=O (156.2 ppm), C=N (148,7 ppm) and OCH_3 (55.7 ppm). The peaks centered at 158.1, 132.1, 125.8, 122.0, 120.9 are due to Ar-C2, Ar-C4, Ar-C6, Ar-C5, Ar-C1, respectively. The signals observed in-between 25-50 ppm are attributed to the exploited solvent (DMSO).

Optical absorption and magnetic investigation

The electronic spectral bands for the oxaloylhydrazones and their manganese complexes in DMF solvent have been given in Table 2. The electronic spectra of the investigated ligands shows peaks at 350-392, 338-375, 306-340, 292-315 and 280-303 nm due to (n-π*, C=N), (n-π*, C=O), (π-π*, C=N), (π-π*, C=O) and (π-π*, aromatic ring), respectively. The proposed

geometry of the isolated complexes was deduced from the electronic spectra in DMF and magnetic measurements. The optical absorption spectrum of I revealed two absorptions at 460 and 425 nm assigned to $^6S \rightarrow {}^4G$ and ^4P transitions, respectively. The observation of these bands suggests a tetrahedral environment around the Mn^{2+} ion [43]. The electronic spectra of II showed two weak bands at 430 and 380 nm assignable to $^6A_{1g} \rightarrow {}^4T_{1g}(G)$ and $^4T_{2g}(G)$ transitions, respectively, considering an octahedral configuration around the Mn^{2+} ions [44]. Other bands attributed to octahedral ($^6A_{1g} \rightarrow {}^4E_g$, $^4A_{1g}$, $^4T_{2g}(D)$ and $^4E_g(D)$) and tetrahedral ($^6S \rightarrow {}^4D$ and ^4F) structures of Mn^{2+}-complexes are overlapped with strong ligand bands [44].

The room temperature magnetic moments (μ_{eff}, Table 1) of manganese complexes under study supported the proposed stereochemistry derived from the electronic data [44]. The μ_{eff} values of compounds I and II, measured at 4 and 6 amperes (A), are close to spin only value and refer to high spin complexes. In other words, the results point to the presence of 5 unpaired electrons in both complexes confirming a paramagnetic nature and illustrating that Mn^{2+} ions were not oxidized by dihydrazone ligands.

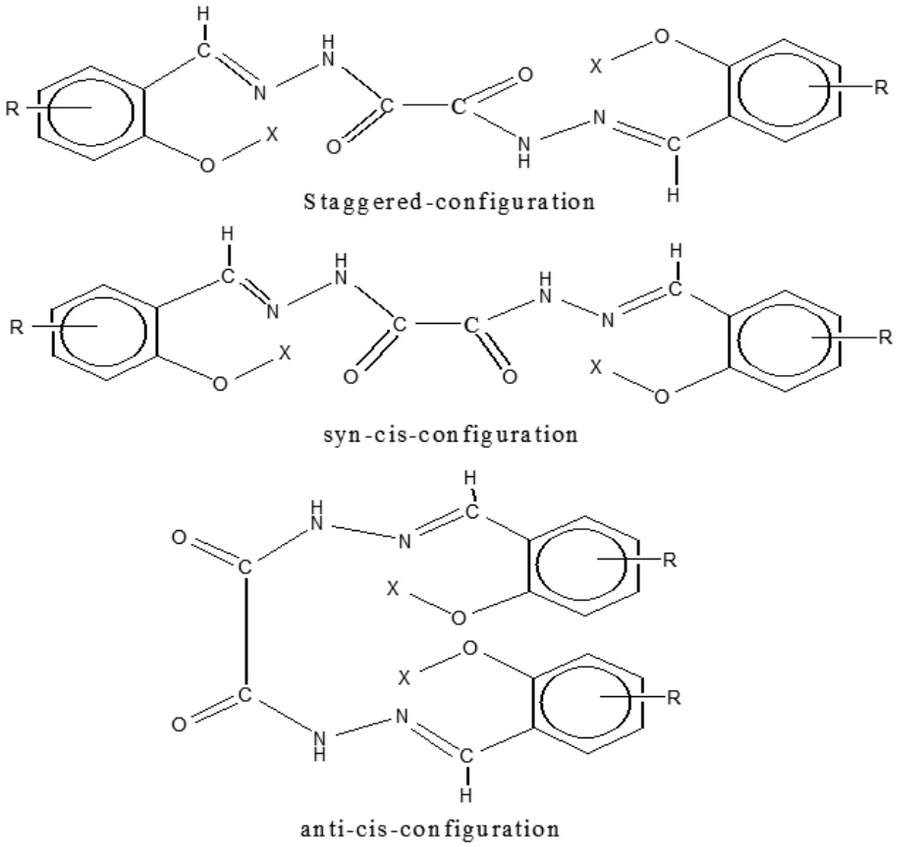

Fig. 2. Proposed structures of oxaloyldihydrazone ligands:
Where L_1 (R=ph, X=H), and L_2 (R=H, X=CH_3).

Table 3: Corrosion parameters for aluminum coupons in (1M HCl) solution in presence and absence of different concentrations of hydrazone ligands obtained from weight loss measurement at room temperature after 4 hrs immersion time.

Inhibitor	Conc. (M)	Weight Loss (g)	Rate of corrosion mg cm^{-2} h^{-1}	θ	Inhibition efficiency η %
L_1	Blank	0.0210	0.0070	-	-
	5×10^{-4}	0.0139	0.0046	0.34	34
	1×10^{-4}	0.0153	0.0051	0.27	27
	5×10^{-5}	0.0163	0.0054	0.22	22
	1×10^{-5}	0.0178	0.0059	0.15	15
L_2	Blank	0.0188	0.0063	-	-
	5×10^{-4}	0.0067	0.0022	0.64	64
	1×10^{-4}	0.0084	0.0029	0.54	54
	5×10^{-5}	0.0099	0.0035	0.44	44
	1×10^{-5}	0.0114	0.0038	0.39	39

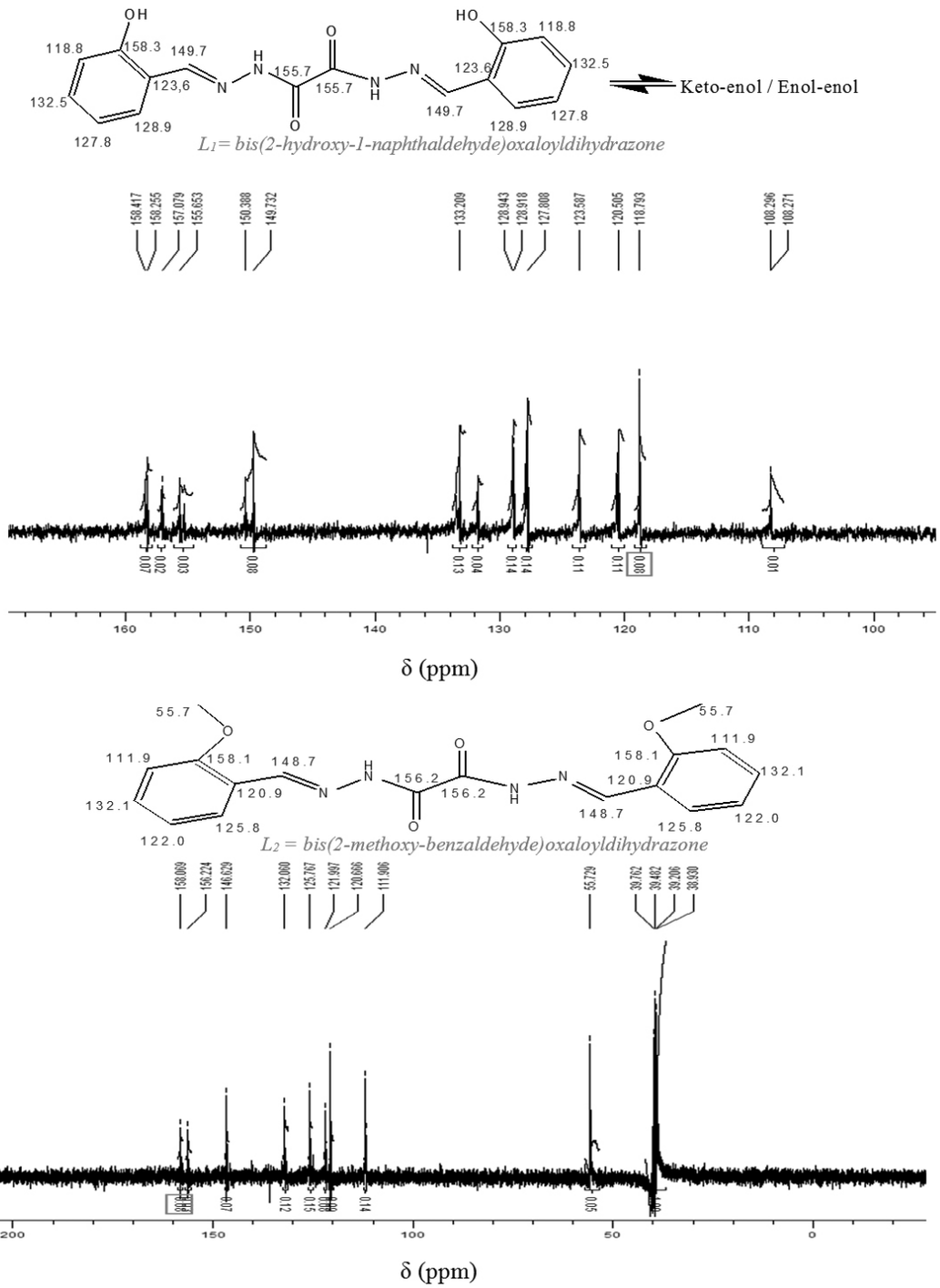

Fig. 3. ^{13}C NMR spectra of L_1 and L_2 in DMSO-d_6 at RT.

Thermogravimetric analysis

The thermogram (TGA) data of complex I exhibited five steps of decomposition. The first step (50-150 °C) corresponds to the loss of 1/2 H_2O-crystalline (found/calculated % = 2.0/1.7), while the other four stages are related to the gradual decomposition of the complex with formation of speculated metal oxides at the final step. TG of II gave four stages of decomposition. The first one (140-280 °C) is attributed to the loss of $2OAc^-$ groups (found/calculated% = 18.0/17.5) while the other three stages (300-380, 400-550, 600-800 °C) concerned to the gradual decomposition of the complex with formation of MnO at the final stage (found/calculated % =11.1/10.5).

On the basis of the various physico-chemical and spectral studies presented above and their discussion, the complexes may be suggested to have structures shown in Fig. 4

Electron paramagnetic resonance (EPR)

The complexes I and II have been analyzed by EPR spectroscopy at room temperature and their spectra are shown in (Fig. 5). The ground state of both octahedral and tetrahedral d^5 ion (spin free) is ^{6}A. The energy levels are at ±5/2, ±3/2, ±½ and a single isotropic resonance at g = 2 is easily attained.

Accordingly, the EPR spectra of complexes I and II exhibited one broad signals with two "g" values ($g_{//}$ $g_{\perp}$), Table 1. The absence of hyperfine splitting for these complexes ruled out any axial distortion. The average g values were calculated using the formula:

$$g_{av.} = \frac{1}{3\left[g_{//} + 2g_{\perp}\right]}$$

Where, the calculated values are inserted also in Table 2.

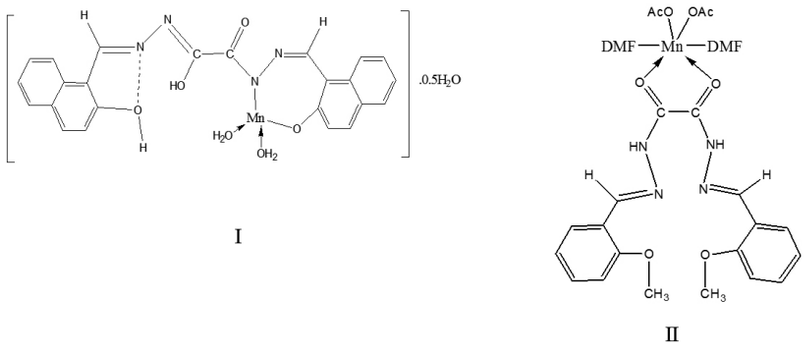

Fig. 4. Suggested structures of Mn^{II}-oxaloyldihydrazone complexes.

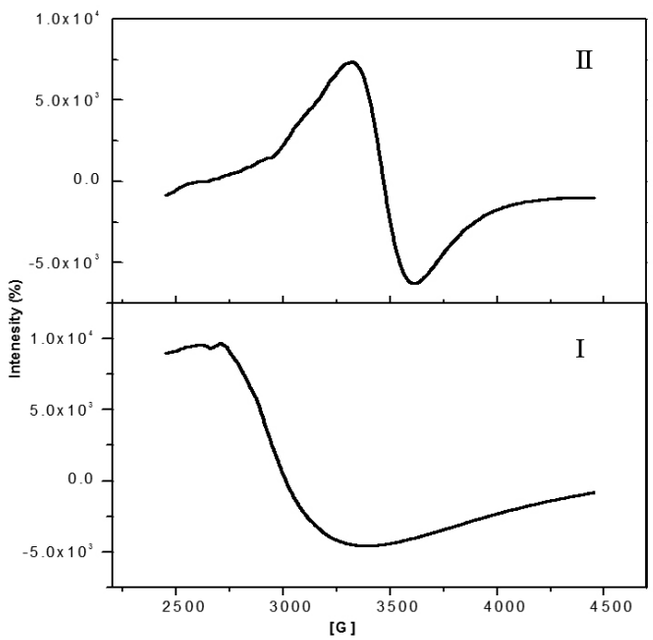

Fig. 5. The plots of $(\alpha h\upsilon)^2$ vs. $h\upsilon$ of Mn(II)-oxaloyldihydrazone complexes.

The average g values (g_{av}) of I and II complexes are nearly 1.9 close to free electron g value indicating the absence of spin-orbit coupling. The $g_{//}$ is a moderately function for covalent character. The complexes I and II exhibited $g_{//}$ at 1.930 and 1.998, respectively which are less than 2.3, implying covalent nature of manganese-ligand bond in the present complexes, where, $g_{//}$>2.3 is character of ionic metal-ligand bond [45,46]. Fairly high values of g are in conformity with the oxygen and nitrogen coordination in these compounds [18].

Optical band gape energy

The energy band gap of the ligands and their manganese complexes has been calculated with the help of absorption spectra. To calculate the optical band gap energy from absorption spectra, Tauc's relation is used [30,31]:.

$$\alpha h\nu = A\left(h\nu - E_g\right)^m$$

Where hν is the photon energy, h is Planck's constant, α is the absorption coefficient, E_g is the optical energy gap, A is the constant, m is equal to 1/2 and 2 for direct and indirect transitions, respectively. The absorption coefficient (α) was calculated from to the relation:

$$\alpha = \frac{1}{d\ln\left(1/T\right)}$$

Where d is the width of the cell and T is the measured transmittance.

We plot a graph between $(\alpha h\upsilon)^2$ versus hν, the extrapolation of the straight line to $(\alpha h\upsilon)^2 = 0$ axis gives optical band gap. Figure 6 shows Tauc's plot for all the samples. Band gap for ligands and Mn^{2+}-complexes in DMF solvent lies in the ranges 3.06-3.42 eV and 2.38-3.39 eV, respectively and are mentioned in Table 1. Careful inspection of Table 1 shows that the optical band gap values of the two ligands (E_g) are minimized upon complexation. This reduction in band gap is attributed to the mobilization of the electrons toward the metal [47]. It is suggested that the manganese raises mobilization of the ligand electrons by

accepting them in its shell thus the width of the localized levels in the resulting complex is expanded and in turn, the band gap is smaller. This result has many applications in optics, electronics and energy conversion devices [48]. In fact small band gap facilitates electronic transitions between the HOMO-LUMO energy levels and makes the molecule more electro-conductive [49]. From the observed values of optical properties, it is seen that the synthesized compounds lie in the same range of highly efficient photovoltaic materials [47,50] and can be used as semiconductors.

Table 4: Values of ΔG_{ads} (kJ/mol), adsorption constant (K), Freundlich heterogeneity factor (n), lateral interaction term describing the interaction in adsorbed layer (α), and correlation coefficient (R^2) of inhibitors for aluminum coupons.

Ligands	Freundlich isotherm					Langmuir isotherm			Frumkin isotherm			
	1/n	n	K_{ads} ($molL^{-1}$)	ΔG_{ads} (kJ mol^{-1})	R^2	K_{ads} ($molL^{-1}$)	ΔG_{ads} (kJ mol^{-1})	R^2	α	K_{ads} ($molL^{-1}$)	ΔG_{ads} (kJ mol^{-1})	R^2
L_1	0.207	4.83	2.5420	-12.39	0.9767	1.6994	-11.38	0.9984	6.471	0.00013	-12.32	0.8287
L_2	0.129	7.75	1.2680	-10.65	0.9624	1.7006	-11.38	0.9991	3.539	0.00044	-9.29	0.9588

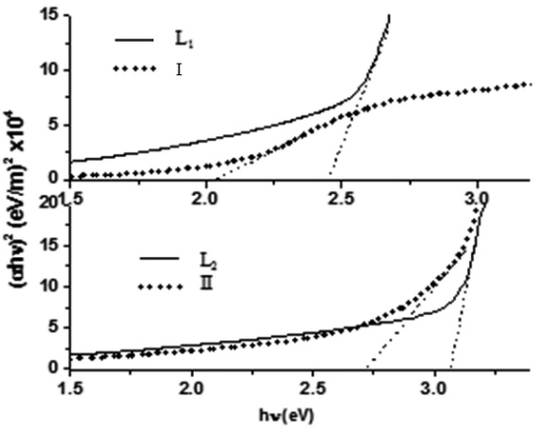

L_1= bis(2-hydroxy-1-naphthaldehyde)oxaloyldihydrazone,

L_2 = bis(2-methoxy-benzaldehyde)oxaloyldihydrazone,

I = Mn^{2+}-bis(2-hydroxy-1-naphthaldehyde)oxaloyldihydrazone and

II = Mn^{2+}-bis(2-methoxy-benzaldehyde)oxaloyldihydrazone

Fig. 6. The efficiency for aluminum coupons in 1M HCl solution in the presence and absence of different concentrations of oxaloyldihydrazone ligands at room temperature.

Weight loss studies

The inhibitive actions of ligands on the dissolution of aluminum in 1 M HCl are investigated (Table 3). Careful inspection of these results showed that, by increasing the inhibitor concentration, both (θ) and (η%) are increased while the weight loss is reduced. So, the dissolution of aluminum in the presence of the investigated inhibitor can be interpreted on the basis of interface inhibition mode where the adsorbed species mechanically screen the coated part of the metal surface from the action of the corrosive medium. This adsorption is related to some discriminated features of the investigated oxaloyldihydrazones like the functional groups (OH, NH, C=O and C=N), quite large molecular size, high molecular weight, aromaticity, electron density at the donor atoms (N:, :O:) and also the π-orbital character of the azomethine, carbonyl and phenyl groups. Adsorption and desorption of inhibitor molecules continuously occur at the metal surface and an equilibrium exists between the two processes at a particular temperature. The inhibition achieved by dihydrazone compounds decreases in the sequence $L_2 < L_1$ and this behavior can be discussed on the basis that the methoxy group (in L_2) is more electron donating group than naphthoic hydroxyl (in L_2). Positive mesomeric effect (+M effect) and negative inductive effect (–I effect) of -OCH_3 lead to push the electron density toward the donor atoms of O=C-NH-N=CH part via the phenyl ring as a result of delocalization and subsequently enhance the bond strength between the molecule and the corroding aluminum surface. Under these circumstances, the inhibition efficiency of (L_2) should be higher than that of L_1. Furthers, existence of two naphthyl rings in the structure of L_1 may cause crowding that encourages incomplete coating besides they can withdraw the electron pair of ortho-OH group toward themselves under the influence of resonance phenomenon. The iinhibition efficiency values of the dihydrazone are set out in Table 3 whereas the maximum protection efficiency percentages of L_1 is 34% while that for L_2 is 64%. The obtained data boosts the application of L_2 as plausible corrosion pickling inhibitor. It is evident that the inhibition efficiency values is not extremely high owing to the lower ligand concentrations used.

Kinetic treatment

Spontaneous corrosion reaction is a heterogeneous one, composed of anodic and cathodic reactions with the same rate. On this basis the kinetic analysis of the data is considered necessary. In the present work, the initial weight of aluminum coupon at time t is designated as W_i, the weight loss is ΔW and the weight change at time t is (W_i - ΔW) or W_f. When logW_f was plotted versus time, a linear variation was remarked (Fig. 7) considering a first order reaction [51]:

$$\log W_f = \log W_i - Kt$$

Where: W_i = the initial weight before immersion, K = slope (the rate constant), and t is time.

From the rate constant values obtained from the graphs, regarding the adsorption reaction on manganese surface proceeds as first order, the half-life values ($t_{½}$) of the metal in the test solutions were calculated using the equation [51]:

$$t_{1/2} = \frac{\ln 2}{K} = \frac{0.693}{K}$$

Adsorption isotherms and Gibb's free energy

The adsorption behavior of oxaloydihydrazones on the surface of aluminum was studied by fitting data calculated for the degree of surface coverage to different adsorption isotherms such as Freundlich, Temkin, Langmuir, Frumkin, and Flory-Huggins. The obtained correlation coefficients (R^2) were used to determine the best fits [52]. The Gibb's free energy of adsorption ΔG_{ads} at room temperature, which can characterize the interaction of adsorbed molecules and aluminum surface, for all choice isotherms was calculated using the formula [53]:

$$\Delta G_{ads} = -RT \ln 55.5 K_{ads}, \quad where: T \ is \ the \ temperature \ (in \ K)$$

Freundlich isotherm

Freundlich isotherm can be expressed according to the equation [54],

$$\ln\theta = \ln K_{ads} + \frac{1}{n}\ln C$$

Where C is the inhibitor bulk concentration in mol/L, K_{ads} ($mol^{-1}L$) is the equilibrium constant of adsorption and n is Freundlich heterogeneity factor.

Plots of lnθ versus lnC of all ligands (Fig. 8) were linear with acceptable correlation coefficient which illustrate the applicability of Freundlich isotherm. The thermodynamic parameters obtained for the Freundlich adsorption isotherm were recorded in Table 4. This demonstrates that values of the adsorption parameter n are greater than unity implying favored adsorption process [55].

Langmuir adsorption

The assumption establishing Langmuir adsorption isotherm is given by the equation [56],

$$\frac{C}{\theta} = \frac{1}{K} + C$$

Where: C is the concentration of the inhibitor in the bulk electrolyte, θ is the degree of surface coverage of the inhibitor and K is the equilibrium constant of adsorption of the inhibitor. Plotting of logC/θ against logC at 301 K (Figure 8) for the two inhibitors gave straight lines with high correlation coefficients (very close to unity) indicating that Langmuir adsorption isotherm is applicable to the adsorption of oxaloylhydrazones on the surface of aluminum. Values of Langmuir parameters deduced from the isotherms are recorded in Table 4. The application of Langmuir isotherm to the adsorption of oxaloylhydrazones on surface of aluminum indicated that there is no interaction between the adsorbate and adsorbent. The equilibrium constant (K) of the adsorption process can be calculated from the reciprocal of anti logarithm of the intercept.

Frumkin adsorption

Frumkin adsorption isotherm can be represented by the equation [57],

$$\log C\left[\frac{\theta}{1-\theta}\right] = 2.303\log K + 2\alpha\theta$$

Where: K is the adsorption-desorption constant and α is the lateral interaction term describing the interaction in adsorbed layer.

Plots of logC[θ/(1-θ)] versus θ shown in Fig. 8 were linear with acceptable correlation coefficients suggesting that the adsorption of oxaloylhydrazones on the aluminum obeys Frumkin isotherm. The values for Frumkin adsorption parameters are listed in Table 4. It is of interest to note that, the positive α values reflect the attractive behavior of the inhibitor on the surface of aluminum [58].

Adsorption consideration

The inhibition effect of inhibitor compound is ascribed to adsorption of the molecule on metal surface. This adsorption may be physical or chemical depending on the adsorption strength. For a physical adsorption mechanism, the value of the free energy (ΔGads,) of adsorption should be less negative than -40 kJ/mol required for chemical adsorption. The negative values of ΔG_{ads} set out in Table 4 indicate that the adsorption of oxaloylhydrazones on aluminum surface is spontaneous and in the same time it characterizes their strong interaction with the metal surface [59]. Moreover, the magnitudes of ΔG_{ads} are in good agreement with physical adsorption mechanism [59]. Accordingly, the prohibition mechanism is due to the formation of a protective film on the metal surface where the additive covers both the anodic and cathodic sites.

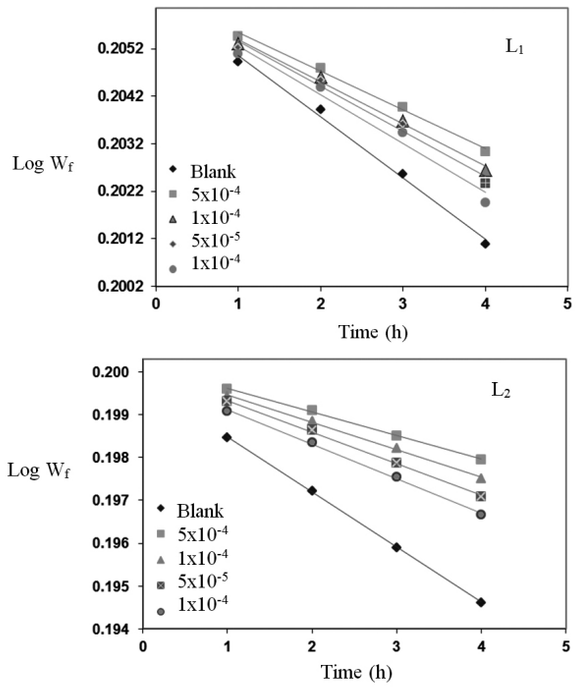

Fig. 7. Variation of log W_f with time (hour) for aluminum coupons in HCl solution containing oxaloyldihydrazone ligands (L_1 and L_2).

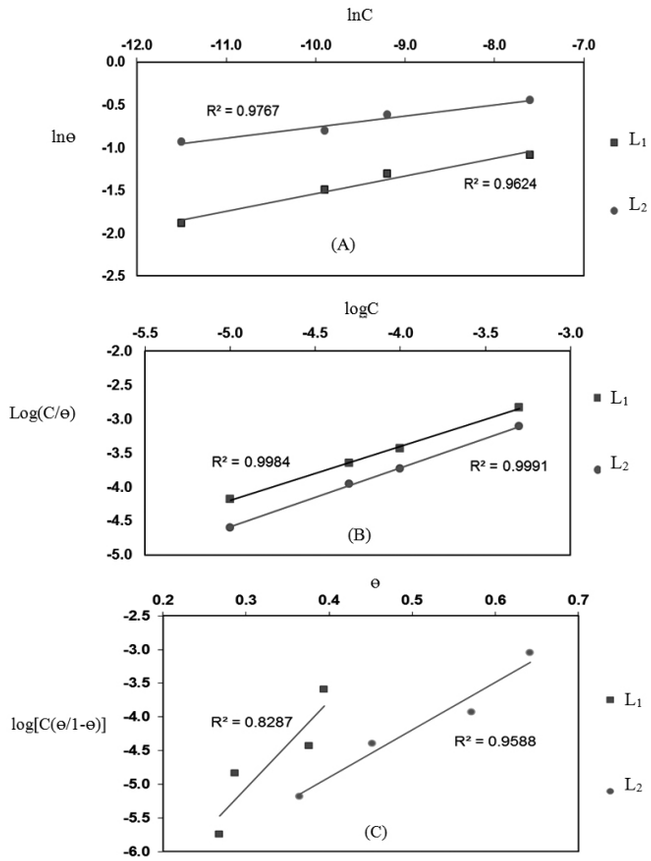

Fig. 8. Plots of Freundlich lnθ vs. lnC (A), Langmuir Log(C/θ) vs. LogC (B), and Frumkin LogC[θ/(1-θ)] vs. θ (C) adsorption isotherms for aluminum coupons in HCl solution containing oxaloyldihydrazone ligands (L_1 and L_2).

CONCLUSION

In the present study, we have prepared two monomeric manganese complexes and characterized them on the basis of data obtained from physicochemical and spectroscopic studies. The oxaloyldihydrazone ligands (L_1 and L_2) can be synthesized by usual condensation of oxaloyldihydrazide with the appropriate aldehyde (2-hydroxynaphthaldehyde and 2-methoxybenzaldehyde) in a 1:2 molar ratio. The stoichiometry of the isolated solid complexes (I, II) is proposed based on the elemental analysis results (CHNM). From the present investigation on the hydrazone complexes, it is evident that, the dihydrazone in complex I functions as a keto-enol bidentate donor through deprotonated secondary NH and naphthoate oxygen giving mononuclear tetrahedral complex. However, in the case of the complex II, it behaves as a diketo bidentate donor within the two carbonyl (C=O) groups providing mononuclear octahedral complex. It can be observed that the band gap of all the samples lies in the range of wide band gap semiconductors. The band gap values of ligands have been minimized upon chelation. Corrosion inhibition results reflect the capability of the two ligands to mitigate the corrosion of aluminum in HCl solution especially L_2 which contains an electron donating methoxy group in its structure. The inhibition efficiency of the ligands was found to increase with increment of the ligand concentration following the trend: $L_2 > L_1$. The obtained negative values of Gibb's free energy indicated that the adsorption of the inhibitor is spontaneous and follows the mechanism of physical adsorption. The experimental data fit well with Freundlich, Langmuir and Frumkin adsorption isotherms.

ACKNOWLEDGEMENT

Corresponding author expresses his gratitude to the scientific research deanship at Jouf University. This work is supported by Jouf University through the research project No. (39/168).

REFERENCES

[1] M. Mohan, N. S. Gupta, M. P. Gupta, A. Kurnar, M. Kurnar, N. K. Jha, Inorg. Chim. Acta. 152, 25, (1988).
[2] P. Barbazan, R. Carballo, B. Covelo, C. Lodeiro, J. C. Lima, E. M. Vazquez-Lopez, Eur. J. Inorg. Chem. 2713 (2008).
[3] A. S. Pedrares, N. Camina, J. Romero, M. L. Duran, J. A. Garcia Vazquez, Polyhedron 27, 3391, (2008).
[4] E. M. Sherif, A. H. Ahmed, Synth. React. Inorg. Met-Org. Chem. 40, 365, (2010).
[5] M. Ghasemian, A. Kakanejadifard, F. Azarbani, A. Zabardasti, S. Shirali, Z. Saki, S. Kakanejadifard, Spectrochim. Acta A 38, 643, (2015).
[6] A. H. Ahmed, E. Ewais, J. Chem. Pharm. Res. 4, 3349 (2012).
[7] J. M. Price, Federation Proc. 20, 223, (1961).
[8] V. P. Singh, A. Katiyar, Pestic. Biochem. Phys. 92, 8, (2008).
[9] V. P. Singh, P. Singh, A. K. Singh, Inorg. Chim. Acta 379, 56, (2011).
[10] A. M. Hassan, A. H. Ahmed, H. A. Gumaa, B. H. Mohamed, A. M. Eraky, J. Chem. Pharm. Res. 7, 91 , (2015) and references therein.
[11] H. Abd El-Wahab, M. Abd El-Fattah, A. H. Ahmed, A. A. Elhenawy, N. A. Alian, J. Organomet. Chem. 791, 99, (2015).
[12] V. Lozan, P.-G. Lassahn, C. Zhang, B. Wu, C. Janiak, G. Rheinwald, H. Lang, Z. Naturforsch. B 58, 1152, (2003).
[13] W. H. Hegazy, Monatsh. Chem. 132, 639 (2001).
[14] R. Dinda, P. Sengupta, S. Ghosh, T. C. W. Mak, Inorg. Chem. 41, 1684, (2002).
[15] R. Raveendran, S. Pal, Polyhedron 24, 57, (2005).
[16] M. Salavati-Niasari, A. Sobhani, J. Mol. Catal. A 285, 58, (2008).
[17] R. A. Lal, S. Adhikari, A. Kumar, J. Chakraborty, S. Bhaumik, Synth. React. Inorg. Met.-Org. Chem. 32, 81 (2002).
[18] R. A. Lal, D. Basumatary, S. Adhikari, A. Kumar, Spectrochim. Acta A 69, 706, (2008).
[19] A. H. Ahmed, Rev. Inorg. Chem. 34, 153 (2014).
[20] A. H. Ahmed, M. S. Thabet, Syn. and Rea. in Ino. and Metal-Org. Chem. 45, 1632, (2015).
[21] A. H. Ahmed, A. G. Mostafa, Mater. Sci. Eng. C 29, 877, (2009).
[22] A. H. Ahmed, M. S. Thabet, J. Mol. Struct. 1006, 527, (2011).
[23] M. S. Thabet, A. H. Ahmed, J. Porous Mater. 20, 319, (2013).
[24] A. H. Ahmed, J. Mol. Struct. 839, 10, (2007).
[25] R. Lopez-Sesenes, J. G. Gonzalez-Rodriguez, M. Casales, L. Martinez, J. C. Sanchez-Ghenno, Int. J. Electrochem. Sci. 6, 1772, (2011).
[26] J. Aljourani, M. A. Golozar, K. Raeissi, Mater. Chem. Phys. 121, 320, (2010).
[27] H. S. Awad, S. A. Gawad, Anti Corros. Meth. Mater. 52, 328. (2005).
[28] E. W. Flick, Corrosion Inhibitors, Park Ridge, New Jersey, 1987.
[29] T. M. Salama, A. H. Ahmed, Z. M. El-Bahy, Micropor. Mesopor. Mater. 89, 251, (2006).
[30] M. M. Rashad, A. M. Hassan, A. M. Nassar, N. M. Ibrahim, A. Mourtada, Appl. Phys. A 117, 877, (2013).
[31] Tauc, J Mater. Res. Bull. 3, 37, (1968).
[32] K. Orubite-Okorosaye, N. C. Oforka, J. Appl. Sci. Environ.Mgt. 8, 57, (2004).
[33] I. A. Mohammed-Dabo, S. A.Yaro, G. Abubakar, S. I. Ayilara, T. U. Apugo-Nwosu, S. A. Akuso, J. Basic. Appl. Sci. Res. 1, 1989, (2011).
[34] R. A. Lal, S. Adhikari, A. Kumar, In. J. Chem. 36A, 1063, (1997).
[35] K. Burger, I. Ruff, F. Ruff, J. Inorg. Nucl. Chem. 27, 179, (1965).
[36] O. B. Chanu, A. Kumar, A. Ahmed, R. A. Lal, J. Mol. Struct. 1007, 257, (2012).
[37] A. M Ali, A. H Ahmed, T. A Mohamed, B. H Mohamed, Transit. Met. Chem. 32, 461, (2007).
[38] S. Salapathy, B. Sahoo, J. Inorg. Nucl. Chem. 32, 2223, (1970).
[39] A. H. Ahmed, A. M. Hassan, H. A. Gumaa, B. H. Mohamed, A. M. Eraky, Journal of Advances in Chemistry 11, 3834, (2015).
[40] D. Kumar, A. Syamal, L. K. Sharma, J. Coord. Chem. 61, 1788, (2008).
[41] A. Kumar, R. A. Lal, O. B. Chanu, R. Borthakur, A. Koch, A. Lemtur, S. Adhikari, S. Choudhury, J. Coord. Chem. 64, 1729, (2011).
[42] K. Nakamoto, Inorganic Spectra of Inorganic and Coordination Compounds, 2Ed, John Wiley & Sons, New York, 1970.
[43] C. Furlani, A. Furlani, J. Inorg. Nucl. Chem. 19, 51, (1961).
[44] F. A. Cotton, G. Wilkinson, Advanced Inorganic Chemistry, 2Ed, Interscience, 1966.
[45] A. B. P. Liver, Inorganic electronic spectroscopy, Elsevier, New York, 1984.
[46] D. Kivelson, R. Nieman, ESR Studies on the Bonding in Copper Complexes, J Chem. Phys. 35, 149, (1961).
[47] F. Karipcin, B. Dede, Y. Caglar, D. Hur, S. Ilican, M. Caglar, Y. Sahin, Opt. Commun. 272, 131, (2007).
[48] N. Turan, B. Gündüz, H. Körkoca, R. Adigüzel, N. Çolak, K. Buldurun, J. Mex. Chem. Soc. 58, 65, (2014).
[49] S. K. Sengupta, O. P. Pandey, B. K. Srivastava, V. Sharma, Transit. Met. Chem. 23, 349, (1998).
[50] M. L. Fu, G. C. Guo, X. Liu, L. Z. Cai, J. S. Huang, Inorg. Chem. Commun. 8, 18, (2005).
[51] P. C. Okafor, E. E. Ebenso, U. J. Ekpe, Int. J. Electrochem. Sci. 5, 978 (2010).
[52] M. Karakus, M. Sahin, S. Bilgic, Mater. Chem. Phys. 9, 561, (2005).
[53] J. Rodosevic, M. Kliskic, L. J. Aljinovic, S. Vuko,.In the Proceedings of the 8th European Symposium on Corrosion inhibition, Ann Univ. ferrara, Italy, 1995, pp: 817.
[54] R. Mohammad, M. Hadj, S. Mina, B. Pourya, J. Appl. Sci. Enviro. Sanit. 6, 1, (2011).
[55] A. L. Ahmad, S. Bhatia, N. Ibrahim, S. Sumathi, Braz. J. Chem. Eng. 22, 1, (2005).
[56] H. Shockry, M. Yuasa, I. Sekine, R. M. Issa, H.Y. El-baradie, G. K. Gomma, Corros. Sci. 40, 2173, (998).
[57] N. O. Eddy, P. Ekwumemgbo, S. A. Odoemelam, Int. J. Phys. Sci. 3, 1, (2008).
[58] H. Ashassi-Sorkhabi, B. Shaabani, B. Aligholipour, D. Seifzadeh, Appl. Surf. Sci. 252, 4039, (2006).
[59] S. Bilgic, M. Sahin, Mater. Chem. Phys. 70, 290, (2001).